Solid State Science and Technology, Vol. 33, No. 2 (2025) 97-107
https://doi.org/10.66514/ssst-33-2-97-107

Structural and Physical Properties of TeO_2-B_2O_3-ZnO Glasses: Evidence of the Mixed-Glass-Former Effect

Nur Baizura Mohamed[1,*], Tengku Fatin Syafiqah Tengku Shahrir[1]
Siti Nasuha Mohd Rafien[2]

[1]*Faculty of Applied Sciences, Universiti Teknologi MARA (UiTM) Pahang Branch, Jengka Campus, 26400 Bandar Tun Razak, Jengka, Pahang, Malaysia*
[2]*Faculty of Applied Sciences, Universiti Teknologi MARA (UiTM) Perak Branch, Tapah Campus, 35400 Tapah Road, Perak, Malaysia*

**Corresponding author (email: nurbaizura620@uitm.edu.my)*

(Received: 1 December 2025 / Revised: 22 December 2025 / Accepted: 24 December 2025 / Published online: 25 December 2025)

ABSTRACT

The mixed-glass-former effect (MGFE) remains one of the most intriguing yet least understood phenomena in glass science, particularly for tellurite-borate systems modified by ZnO. This study aims to unravel the structural and physical origins of the MGFE by investigating a series of $(100 - x)$ $(70TeO_2 - 30B_2O_3) - (x)ZnO$ ($x = 0, 5, 10, 15, 20$ mol%) glasses synthesized via the conventional melt-quenching technique. X-ray diffraction confirmed fully amorphous structures for all samples. FTIR spectra revealed progressive transformation of Te-O-Te linkages into Te-O-B and Zn-O-Te bonds as low frequency band near 930 cm^{-1} shift towards higher wavenumber as increasing ZnO mol%, signifying compositional rearrangement within the glass network. The density, molar volume, and oxygen packing density exhibited non-linear variations at 15 mol% of ZnO content, providing experimental evidence of the MGFE. SEM-EDX analyses verified homogeneous microstructure and uniform elemental distribution, confirming that ZnO was successfully incorporated without phase segregation. These findings demonstrate how ZnO acts as both an intermediate oxide and a network modifier, simultaneously strengthening and depolymerizing the glass framework. The comprehensive correlation between structural and physical parameters provides new insights into the fundamental nature of the MGFE and offers a compositional pathway for designing high-density, optically stable tellurite-borate glasses for photonic applications.

Keywords: Tellurite glass; borate glass; ZnO modifier; mixed-glass-former effect (MGFE); density

INTRODUCTION

Tellurite-based glasses have attracted significant attention due to their excellent infrared transmission, high refractive index, low phonon energy, and suitability for nonlinear optical and photonic applications [1-3]. However, pure TeO_2 glasses suffer from poor chemical durability and thermal instability, which restricts their direct use in devices [4]. Incorporating boron trioxide (B_2O_3) enhances the glass-forming ability, increases network rigidity, and improves resistance to devitrification through the formation of BO_3 and BO_4 structural units [5]. Consequently, tellurite-borate glasses combine the desirable optical characteristics of TeO_2 with the structural stability imparted by B_2O_3 making them promising hosts for infrared components and laser-active materials [6].

When two network formers such as TeO_2 and B_2O_3 coexist, they may interact competitively, producing non-linear variations in density, molar volume, refractive index, and ion transport. This phenomenon is known as the mixed-glass-former effect (MGFE) [7-8]. The MGFE originates from short-range structural competition, including changes in coordination environments and the formation of cross-linking such as Te-O-B, alongside redistribution of bridging and non-bridging oxygens [9]. Although the MGFE has been extensively demonstrated in mixed tellurite-borate and borate-phosphate networks [6,8-11], its structural origin in tellurite-borate glasses, particularly when modified with ZnO remains insufficiently clarified.

Over the past decade, TeO_2-B_2O_3-based glasses modified with alkaline, alkaline-earth or transition-metal oxides have been investigated mostly for their optical absorption, luminescence, frequently involving rare-earth dopants rather than focusing on intrinsic structural changes [12,13]. Only a limited number of studies have examined the undoped ternary TeO_2-B_2O_3-ZnO system and these works have primarily on optical bandgaps [14], radiation shielding behavior or shielding coefficients [15,16] rather than correlating ZnO-induced structural reorganization with density or packing parameters. As a result, the atomic-scale origin of the MGFE in ZnO-modified tellurite-borate glasses remains unresolved, despite its relevance in tuning compactness, network stability, and potential photonic performance. Existing literature demonstrates that ZnO can function both as a modifier and an intermediate oxide, altering glass compactness and oxygen coordination. Yet, a consistent interpretation connecting FTIR structural evolution, density-based physical parameters, and microstructural homogeneity has not been presented. No study to date has comprehensively correlated XRD, FTIR, SEM-EDX, and density-molar volume-OPD parameters in the undoped TeO_2-B_2O_3-ZnO ternary system.

The current study addresses this gap by investigating the influence of ZnO on the structure and physical properties of TeO_2-B_2O_3-ZnO glasses. The primary objective is to correlate vibrational structural changes (from FTIR) and microstructural uniformity (from SEM-EDX) with macroscopic parameters such as density, molar volume, and oxygen packing density. Through this integrated analysis, the study seeks to uncover how ZnO modifies network connectivity and how such modification governs the non-linear physical behavior characteristic of the MGFE. Such a multidiscipline approach, linking XRD, FTIR, SEM-EDX and density-based analyses; offers new insight into the structural dynamics of mixed-former glasses and provides a pathway for designing compositionally optimized tellurite-based materials for optical and photonic applications.

MATERIALS AND METHOD

Glass preparation

A series of ternary glasses with the nominal composition:

$$(100 - x)\,(70TeO_2 - 30B_2O_3) - (x)ZnO\ (x = 0, 5, 10, 15, 20\ mol\%)$$

was prepared by the melt-quenching method. Analytical-grade powders from Sigma Aldrich of TeO_2 (99.99%), B_2O_3 (99.99%) and ZnO (99.99%) were accurately weighed to yield about 7 g per batch. The mixtures were homogenized by milling process for 60 min. The powder mixture was then placed in alumina crucible and heated in a melting furnace at 1000 ^oC for 30 min. High viscosity melt was transferred to annealing furnace at 400 ^oC for 5 h, after quickly cast in a stainless-steel mold in that furnace. The mold was re-heated in the annealing furnace before the super-cooling process was done. The furnace was then turned off and allowed the samples to cool originally to room temperature. All glass samples were stored in desiccator prior to characterization to prevent moisture absorption.

Measurements

Density (ρ) of each glass was determined by the Archimedes' principle using distilled water as the immersion liquid [17]. Each measurement was repeated three times, and the average value was taken with the precision of ±0.001 gcm^{-3}. The molar volume (V_m) and oxygen packing density (OPD) were calculated from:

$$V_m = \frac{M}{\rho} \qquad (1)$$

$$OPD = 1000 \times C\left(\frac{\rho}{M}\right) \qquad (2)$$

where M is the molecular weight of the glass composition [18], ρ is density, C is the number of ions present in the formula unit [19]. Then, glass samples were crushed into fine powder and test for X-ray diffraction (XRD) analysis using a PANalytical X'Pert PRO PW 3040 MPD diffractometer through Cu Kα radiation (λ = 1.5406 Å, 40 kV/40 mA) and scan $2\theta = 10^o$ - 80^o using 0.02 steps. Fourier Transform Infrared (FTIR) spectra (400 – 1200 cm^{-1}) were recorded on a PelkinElmer model Spectrum One FTIR spectrometer, using KBr-pellet technique (32 scans, 4 cm^{-1}). Surface morphology and elemental composition were examined on a TESCAN VEGA Scanning Electron Microscopy (SEM) equipped with an Oxford Instruments energy dispersive X-ray (EDX) detector; samples were gold-sputtered and imaged at 15 kV. All measurements were performed at room temperature; data were processed in OriginPro2024 and Microsoft Excel for statistical verification and plotting.

RESULTS AND DISCUSSION

The variation of density (ρ), molar volume (V_m) and oxygen packing density (OPD) for the $(100 - x)\,(70TeO_2 - 30B_2O_3) - (x)ZnO$ (x = 0, 5, 10, 15, 20 mol%) glass system is summarized in Table 1 and depicted in Figure 1. The measured density values increased from 4.18 gcm^{-3} to 4.52 gcm^{-3}, while the molar volume decreased from 31.16 $cm^3\ mol^{-1}$ to 26.66 $cm^3\ mol^{-1}$ as ZnO concentration increased. This overall densification reflects the higher atomic weight and compactness of Zn^{2+} (ionic radius 0.74 Å) relative to Te^{4+} and B^{3+}, as well as the occupation of interstitial sites within the network.

Table 1. Values of density (ρ), molar volume (Vm) and oxygen packing density (OPD) of (100 – x) (70TeO_2 – 30B_2O_3) – (x)ZnO (x = 0, 5, 10, 15, 20 mol%) glass samples

x (mol %)	$\boldsymbol{\rho}$ (g/cm^3)	$\boldsymbol{V}$m (cm^3/mol)	OPD (mol/l)
0	4.18	31.36	73.80
5	4.33	29.52	74.52
10	4.42	28.37	76.49
15	4.36	28.20	74.83
20	4.52	26.66	76.53

A density anomaly at 15 mol% ZnO, a slight reduction followed by recovery at 20 mol%; marks the mixed-glass-former effect (MGFE), where competing structural rearrangements between TeO_4/TeO_3 and BO_3/BO_4 units cause non-linear packing behavior. Similar anomalies have been reported in other ternary glasses such as Na_2O-B_2O_3-P_2O_5 [10]. The decreasing molar volume trend suggests progressive cross-linking and densification, implying that Zn^{2+}-driven formation of bridging oxygens [20]. In the present system, ZnO does not act as a glass former but instead plays the role of a network modifier with intermediate oxide character. Its influence on the MGFE is indirect and arises from its interaction with the TeO_2-B_2O_3 network. The presence of Zn^{2+} ions facilitates the formation of Zn-O-Te linkages and modifies the distribution of bridging and non-bridging oxygens, thereby altering the structural balance between tellurite and borate sub-networks. This indirect reorganization is reflected in the non-linear physical behavior observed at the MGFE composition. Figure 2 further supports the presence of MGFE, as evidenced by the non-linear variation in oxygen packing density (OPD) with a distinct dip at 15 mol%, reflecting local rearrangements in oxygen coordination within the glass network.

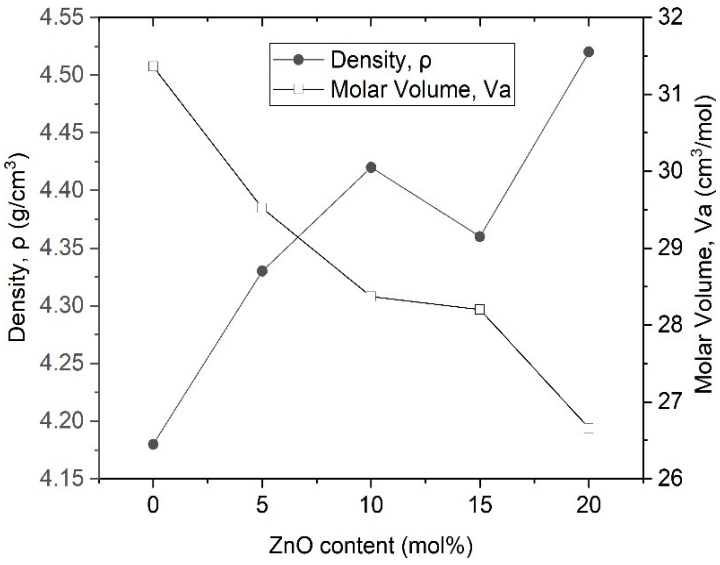

Figure 1. Density (ρ) and molar volume (Vm) of (100 – x) (70TeO_2 – 30B_2O_3) – (x)ZnO (x = 0, 5, 10, 15, 20 mol%) glass samples

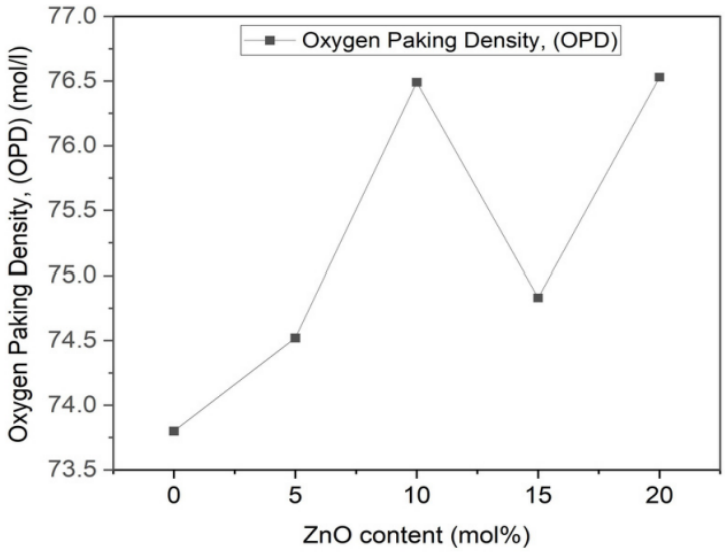

Figure 2. Oxygen Packing Density (OPD) of $(100 - x)$ $(70TeO_2 - 30B_2O_3) - (x)ZnO$ (x = 0, 5, 10, 15, 20 mol%) glass samples

XRD patterns for all compositions shown in Figure 3 display broad humps between $2\theta = 20^o - 35^o$ without any sharp Bragg peaks, verifying complete amorphousness of the quenched samples. This characteristic diffuse halo arises from the absence of long-range atomic order but retention of short-range Te-O and B-O coordination typical of glassy matrices. The absence of crystalline reflections confirms that ZnO was incorporated without forming secondary crystalline phases such as $ZnTeO_3$ or ZnB_2O_5. These results align with findings for similar Zn-containing boro-tellurite systems [21,22], indicating high glass-forming ability and homogeneity.

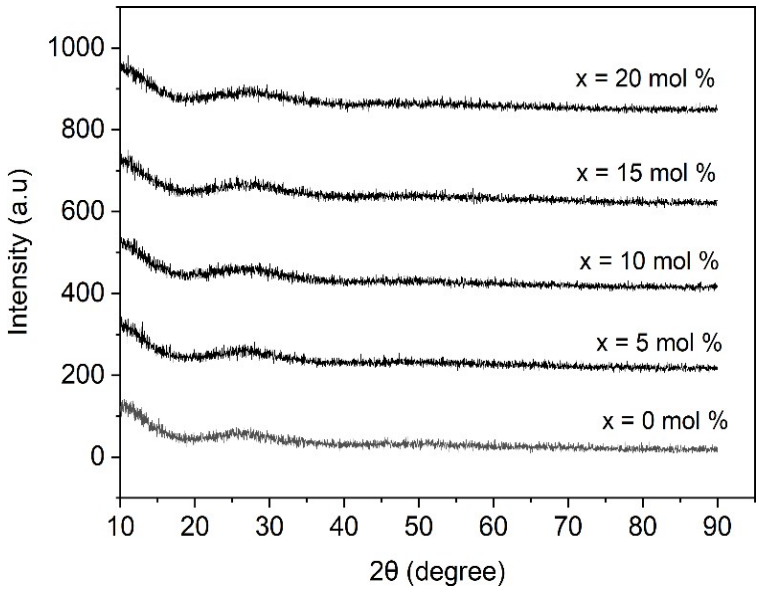

Figure 3. XRD pattern of $(100 - x)$ $(70TeO_2 - 30B_2O_3) - (x)ZnO$ (x = 0, 5, 10, 15, 20 mol%) glass samples

Band assignments are summarized in Table 2, while the FTIR spectra in the range of 400 – 1500 cm^{-1} was exhibited in Figure 4, reveal five principal bands attributed to structural vibrations of Te-O, B-O, and Zn-O groups. It should be noted that, owing to the inherent overlap of vibrational modes in tellurite-borate glass systems, these band assignments are interpreted based on relative shifts and compositional trends rather than exclusive peak attribution.

Table 2. Band assignment of FTIR of glass samples

Band position (cm^{-1})	Assignment	Structural Unit	Oxygen Type
444 – 452	v(Zn-O) stretching	ZnO_4 tetrahedra	BO
664 – 672	v(Te-O) symmetric stretch	TeO_2 (tbp)	BO
754 – 763	v(Te-O) asymmetric stretch	TeO_3 (tp)	NBO
1244 – 1254	v(B-O) stretching	BO_4 tetrahedral	BO
1392 – 1400	v(B-O) stretching	BO_3 trigonal	NBO

A systematic blue-shift of TeO_4 and BO_4 bands with increasing ZnO content implies conversion of non-bridging to bridging oxygen species, enhancing network rigidity. Conversely, red-shift of TeO_3 and BO_3 peaks indicate depolymerization of some unit through Zn^{2+}-O interactions that weaken Te-O-Te and B-O-B bridges. The simultaneous occurrence of both red- and blue-shifts is indicative of the mixed-glass-former effect, wherein modifier cations promote a redistribution of network linkages between tellurite and borate domains rather than affecting each sub-network independently [6]. At higher ZnO level (≥ 15 mol%), the dominant $TeO_4 \rightarrow TeO_3$ transition partially reverses, consistent with densification and OPD recovery. This competition reflects ZnO's dual role: as a network modifier (ZnO_4 units breaking Te-O-Te bonds) and an intermediate oxide (Zn-O-Te bridges forming new linkages), paralleling trends observed by Adamu et al. [23]. Overall, the FTIR evolution confirms a reorganization of both Te and B structural units, underpinning the compositional non-linearity evidenced in density and OPD data.

SEM micrographs exhibited by Figure 5 reveal uniform, pore-free surfaces with no detectable crystalline grains for all compositions, supporting the amorphous XRD patterns. The glass morphology remains smooth and compacts across ZnO substitutions, signifying that melt-quenching produces well-homogenized glasses without micro-phase separation. Comparable microstructures were observed in ZnO-Na_2O-Bi_2O_3-B_2O_3 systems [24] and ZnO-TeO_2-Na_2O glasses [25].

EDX elemental spectra on Table 3 confirms the presence of Te, B, O and ZnO with atomic radius consistent with nominal compositions. The Zn weight percentage increases from 0 to 12.6 wt% as $x = 0 \rightarrow 20$ mol% while Te correspondingly decreases, confirming successful incorporation of ZnO within the glass matrix. The homogeneous elemental mapping images on Figure 6 indicate uniform Zn distribution, evidencing no ZnO clustering or phase segregation – a prerequisite for stable optical and dielectric behavior.

Such homogeneity substantiates the structural reinforcement inferred from density and FTIR results: Zn^{2+} ions occupy interstitial position or replace Te^{4+} in TeO_4 units, generating Te-O-Zn linkages that improve connectivity and chemical durability [20,26].

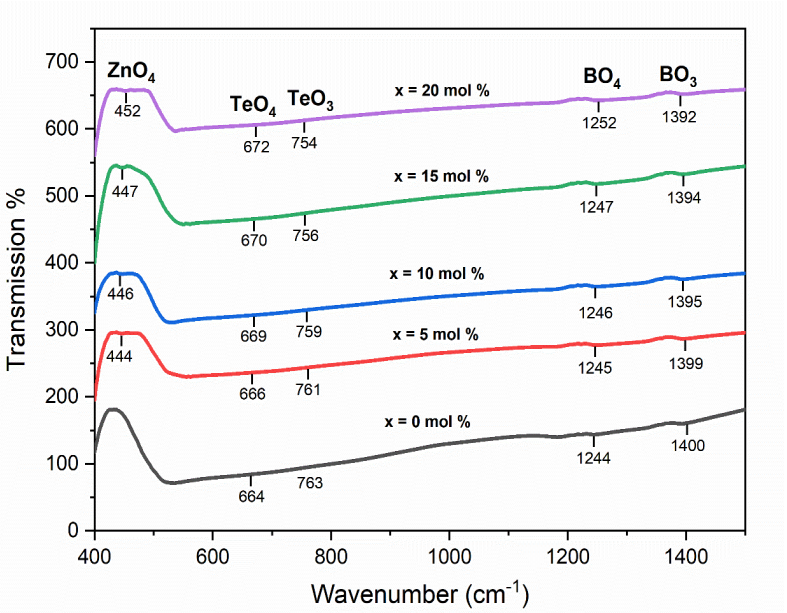

Figure 4. The IR spectra of $(100 - x)$ $(70TeO_2 - 30B_2O_3) - (x)ZnO$ (x = 0, 5, 10, 15, 20 mol%) glass samples

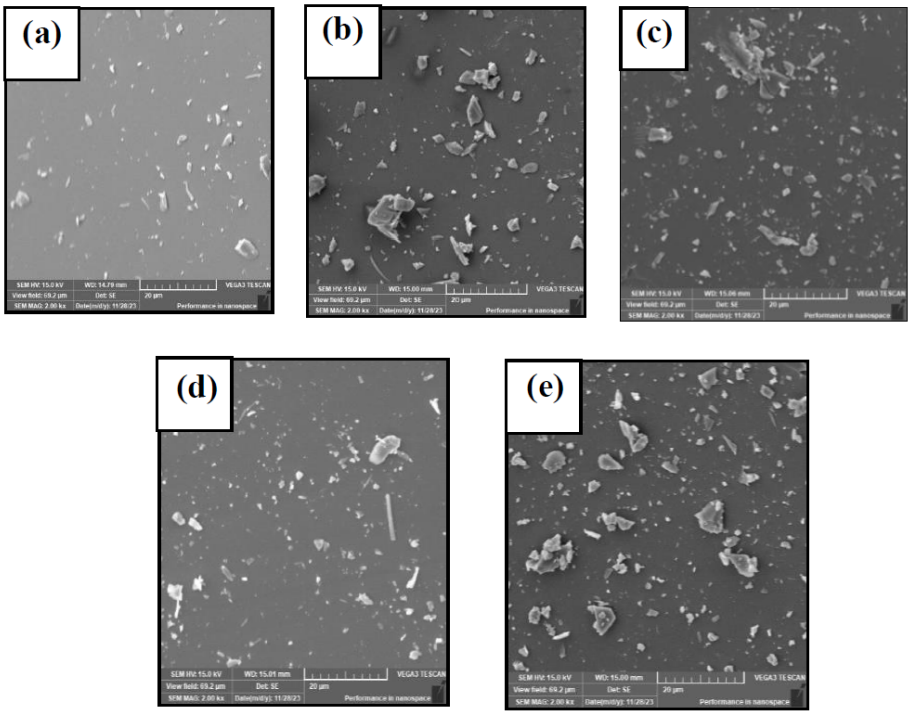

Figure 5. The SEM image of $(100 - x)$ $(70TeO_2 - 30B_2O_3) - (x)ZnO$; x = (a) 0 mol%, (b) 5 mol%, (c) 10 mol%, (d) 15 mol%, and (e) 20 mol% at 2kX

Table 3. Weight percentage of elements of (100 – x) (70TeO_2 – 30B_2O_3) – (x)ZnO (x = 0, 5, 10, 15, 20 mol%) glass measured from EDX analysis

x (mol%)	Weight (%)			
	O	Te	B	Zn
0	25.05	74.30	0.65	-
5	25.63	70.76	0.67	2.94
10	28.86	61.77	2.71	6.67
15	31.97	54.79	3.61	9.62
20	31.08	52.05	4.12	12.57

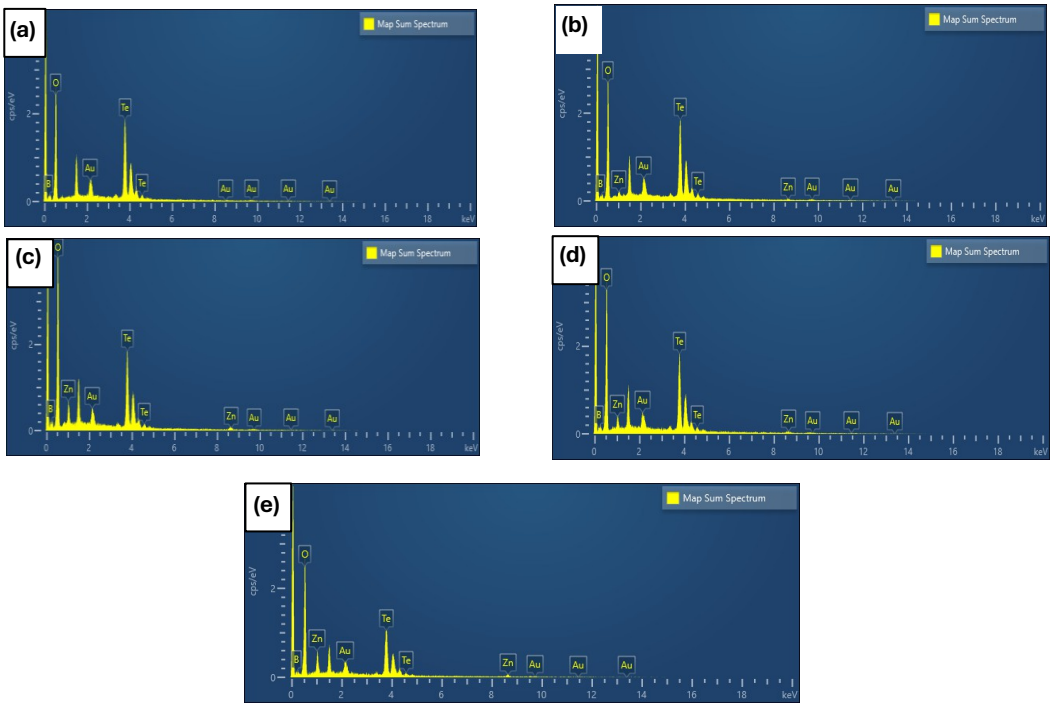

Figure 6. The EDX images mapping of (100 – x) (70TeO_2 – 30B_2O_3) – (x)ZnO; (a) x = 0, (b) x = 5, (c) x = 10, (d) x = 15, and (e) x = 20 mol%) at 20kX

CONCLUSIONS

This work successfully fulfilled the objective of elucidating the structural and physical manifestation of the mixed-glass-former effect (MGFE) in the (100 – x) (70TeO_2 – 30B_2O_3) – (x)ZnO (x = 0, 5, 10, 15, 20 mol%) glass system synthesized by the melt-quenching method. XRD confirmed the amorphous nature of all compositions, while FTIR analysis revealed the transformation of Te-O-Te linkages into Te-O-B and Te-O-Zn bonds through the redistribution of bridging and non-bridging oxygens. The non-linear variations in density, molar volume and oxygen packing density (OPD) indicated particularly the anomaly at 15 mol% ZnO, thus providing clear evidence of MGFE arising from the competitive structural rearrangement between tellurite and borate sub-networks. SEM-EDX observations further verified homogeneous morphology and uniform

elemental dispersion, affirming successful Zn incorporation without phase segregation. Collectively, these results demonstrate that ZnO acts as both intermediate and a modifier oxide, enhancing compactness at low concentrations and inducing transient depolymerization at the MGFE composition. By establishing a direct correlation between structural, microstructural and physical parameters, this study closes the existing gap in understanding the intrinsic origin of MGFE in ZnO-modified tellurite-borate glasses and provides a compositional strategy for developing mechanically robust and optically stable tellurite-based materials for advanced photonic and infrared applications.

ACKNOWLEDGEMENTS

The authors would like to express their sincere appreciation to the Faculty of Applied Sciences, Universiti Teknologi MARA (UiTM), Pahang Branch, Jengka Campus and UiTM Shah Alam, for providing the research facilities and technical assistance.

AUTHOR'S CONTRIBUTION STATEMENT

Conceptualization, N.B.M. and T.F.S.T.S.; Methodology, T.F.S.T.S. and N.B.M.; Analysis and investigation, T.F.S.T.S. and N.B.M; Validation, N.B.M. and S.N.M.R.; Data curation, T.F.S.T.S.; Writing – Original Draft Preparation, N.B.M.; Writing – Review & Editing, N.B.M.; Visualization, N.B.M. and T.F.S.T.S.; Supervision, N.B.M. and S.N.M.R.; Project Administration, N.B.M.

CONFLICT OF INTEREST

The authors declare no conflict of interest.

REFERENCES

1. El-Mallawany RAH, *Tellurite Glasses Handbook: Physical Properties and Data. Second Edition*. CRC Press, Boca Raton; 2012.
2. Patra P, Annapurna K. Transparent tellurite glass-ceramics for photonics applications: A comprehensive review on crystalline phases and crystallization mechanisms. *Progress in Materials Science.* 2022;125:100890.
3. Komatsu T, Dimitrov V. Features of electronic polarizability and approach to unique properties in tellurite glasses. *International Journal of Applied Glass Science*. 2020;11(2):253-271.
4. Sharmin N, Hasan MS, Parsons AJ, Furniss D, Scotchford CA, Ahmed I, Rudd CD. Effect of boron addition on thermal, degradation, and cytocompatibility properties of phosphate-based glasses. *BioMed Research International.* 2013;2013(1):902427.
5. Lu X, Du J. Effect of boron oxide on the structure, properties and bioactivities of bioactive glasses: A review. *Journal of Non-Crystalline Solids: X.* 2022;16:100118.
6. Shuhaimi SA, Hisam R, Yahya AK. Effects of mixed glass former on AC conductivity and dielectric properties of $70[xTeO_2+(1-x)B_2O_3]+15Na_2O+15K_2O$ glass system. *Solid State Sciences*. 2020;107:106345.

7. Raguenet B, Tricot G, Silly G, Ribes M, Pradel A. Revisiting the 'mixed glass former effect' in ultra-fast quenched borophosphate glasses by advanced 1D/2D solid state NMR. *Journal of Materials Chemistry*. 2011;21(44):17693-17704.
8. Christensen R, Olson G, Martin SW. Structural studies of mixed glass former $0.35Na_2O+0.65[xB_2O_3+(1-x)P_2O_5]$ glasses by Raman and ^{11}B and ^{31}P magic angle spinning nuclear magnetic resonance spectroscopies. *Journal of Physical Chemistry B*. 2013;117(7):2169-2179.
9. Christensen R, Olson G, Martin SW. Ionic conductivity of mixed glass former $0.35Na_2O+0.65[xB_2O_3+(1-x)P_2O_5]$ glasses. *Journal of Physical Chemistry B*. 2013;117(51):16577-16586.
10. Christensen R, Byer J, Olson G, Martin SW. The densities of mixed glass former $0.35Na_2O+0.65[xB_2O_3+(1-x)P_2O_5]$ glasses related to the atomic fractions and volumes of short range structures. *Journal of Non-Crystalline Solids.* 2012;358(3):583-589.
11. Christensen R, Byer J, Olson G, Martin SW. The glass transition temperature of mixed glass former $0.35Na_2O+0.65[xB_2O_3+(1-x)P_2O_5]$ glasses. *Journal of Non-Crystalline Solids.* 2012;358(4):826-831.
12. Hasnimulyati L, Halimah MK, Zakaria A, Halim SA, Ishak M, Eevon C. Structural and optical properties of Tm_2O_3-doped zinc borotellurite glass system. *Journal of Ovonic Research.* 2016;12(6):291-299.
13. Hazlin MNA, Halimah MK, Muhammad FD, Faznny MF. Optical properties of zinc borotellurite glass doped with trivalent dysprosium ion. *Physica B*. 2017;510:38-42.
14. Ayuni JN, Halimah MK, Talib ZA, Sidek HAA, Daud WM, Zaidan AW, Khamirul AM. Optical properties of ternary TeO_2-B_2O_3-ZnO glass system. *IOP Conference Series: Materials Science and Engineering*. 2011;17:012027.
15. Süsoy Doğan G. Lithium-boro-tellurite glasses with ZnO additive: Exposure buildup factor (EBF) and nuclear shielding properties. *Avrupa Bilim Ve Teknoloji Dergisi.* 2020;18:531-544.
16. Sayyed MI, Yasmin S, Almousa N, Elsafi M. The radiation shielding performance of polyester with TeO_2 and B_2O_3. *Processes*. 2022;10(9):1725.
17. Alrowaili ZA, El-Hamalawy AA, Ahmmad SK, Bhadra Lasya SVS, Al-Buriahi MS, Rammah YS. A closer-look at lithium strontium boro-fluoride glasses doped with CeO_2 and Yb_2O_3 ions: Synthesis, radiation shielding properties, and prediction of density using artificial intelligence techniques. *Optical Materials.* 2023;135:113338.
18. Ahmed AA, Mawlud SQ. Physical and optical properties of ternary lead-bismuth tellurite glass. *Heliyon*. 2023;9(6):e16730.
19. Rao PSG, Siripuram R, Sripada S. Structural and optical properties of TeO_2-SeO_2-Na_2O glass system. *Indian Journal of Pure & Applied Physics.* 2020;58:50-62.
20. Arora R, Kaur N, Singh H, Kumar D, Bhatia V, Singh SP. B_2O_3-TeO_2-ZnO-Na_2O-Nd_2O_3 glass matrices: A comprehensive study of physical, structural, optical, and thermoluminescence properties. *Materials Chemistry and Physics.* 2024;313:128783.
21. Pandarinath MA, Upender G, Rao KN, Babu DS. Thermal, optical and spectroscopic studies of boro-tellurite glass system containing ZnO. *Journal of Non-Crystalline Solids.* 2016;433:60-67.

22. Effendy N, Sidek HAA, Halimah MK, Zaid MHM, Wahab SAA. Ultrasonic and artificial intelligence approach: Elastic behavior on the influences of ZnO in tellurite glass systems. *Journal of Alloys and Compounds*. 2020;835:155350.
23. Adamu SB, Halimah MK, Chan KT, Muhammad FD, Nazrin SN, Tafida RA. Eu^{3+} ions doped zinc borotellurite glass system for white light laser application: Structural, physical, optical properties, and Judd-Ofelt theory. *Journal of Luminescence*. 2022;250:119099.
24. Parameswarlu B, Rajam B, Vijaykanth A. Synthesis and characterization of ZnO-Na_2O-Bi_2O_3-B_2O_3 glass system. *International Research Journal of Engineering and Technology*. 2022;9(3):683-686.
25. Bairagi S, Bartwal KS, Dhiman SK, Mahajan SK, Ansari GF. Studies on optical and electronic characteristics of ternary zinc-tellurite glasses with varying Zn doping concentration. *Materials Today: Proceedings*. 2023;80:427-433.
26. Effendy N, Sidek HAA, Halimah MK, Zaid MHM. Enhancement on thermal, elastic, optical properties of new formulation tellurite glasses: Influence of ZnO as a glass modifier. *Materials Chemistry and Physics*. 2021;273:125156.